

Supplemental Figures

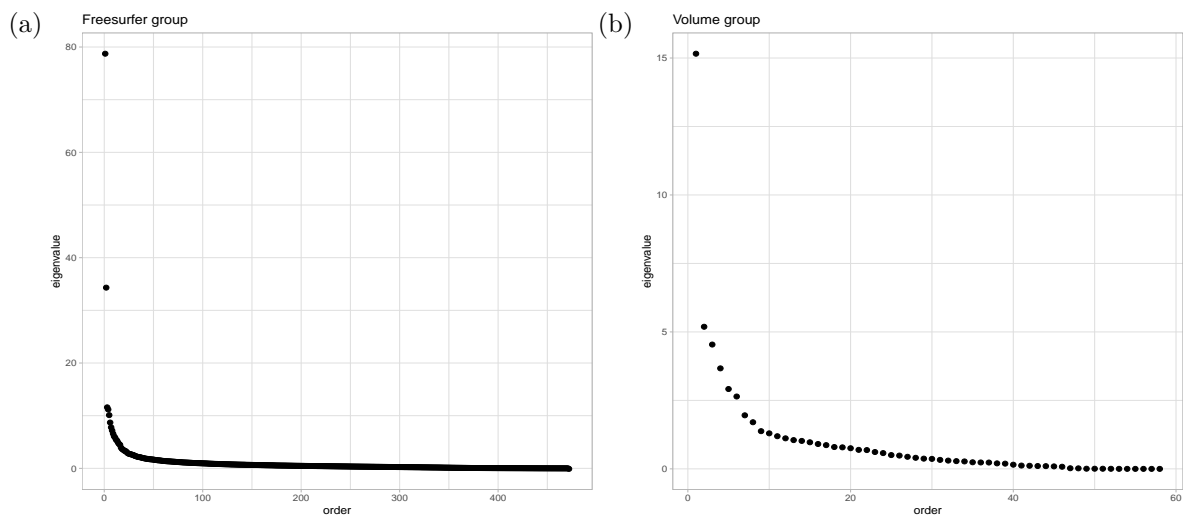


Figure S1: **Eigenvalues of the estimated trait correlation matrix.**

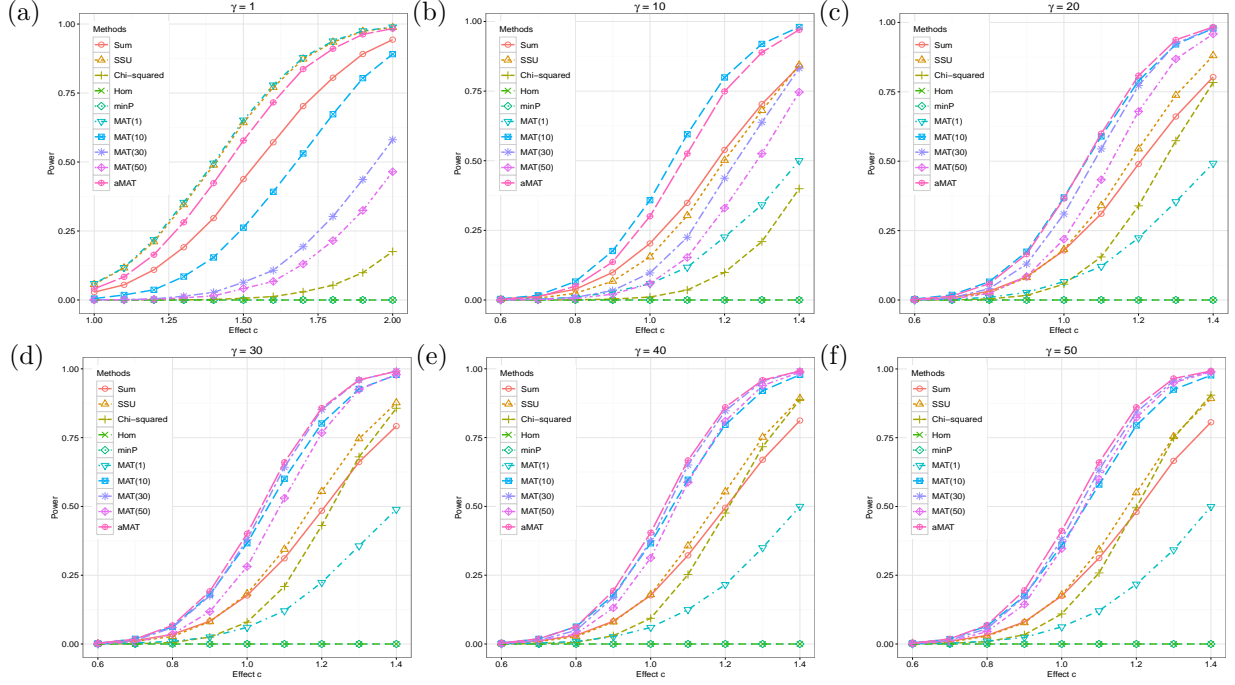


Figure S2: **Empirical power comparison with true Volume trait correlation matrix.** Under the alternative, we generated $\Delta = \sum_{j=1}^k c\sigma_j u_j$, where u_j is the informative singular vector of the Volume correlation matrix \mathbf{R} , c is the effect size and k is the largest integer that stratifies $\sigma_1/\sigma_k < \gamma$. Empirical power was estimated as the proportions of p -values less than significance level 5×10^{-8} . Competing methods including SUM [1], SSU [2, 3], Chi-squared test, Hom [4] test, MAT(1) [5], and minP test [6] have been briefly described in Methods.

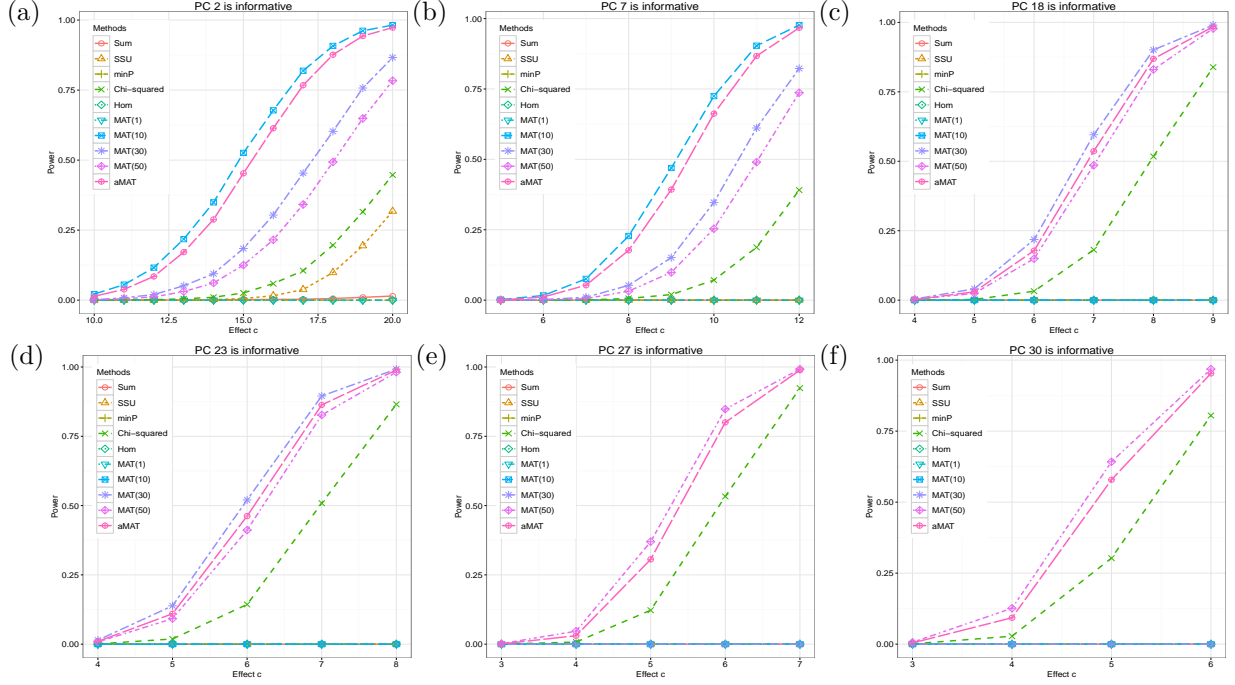


Figure S3: **Empirical power comparison with true Volume trait correlation matrix.** Under the alternative, we generated $\Delta = cu_j$, where u_j is the informative singular vector of the Volume correlation matrix \mathbf{R} , c is the effect size. Empirical power was estimated as the proportions of p -values less than significance level 5×10^{-8} . Competing methods including SUM [1], SSU [2, 3], Chi-squared test, Hom [4] test, MAT(1) [5], and minP test [6] have been briefly described in Methods.

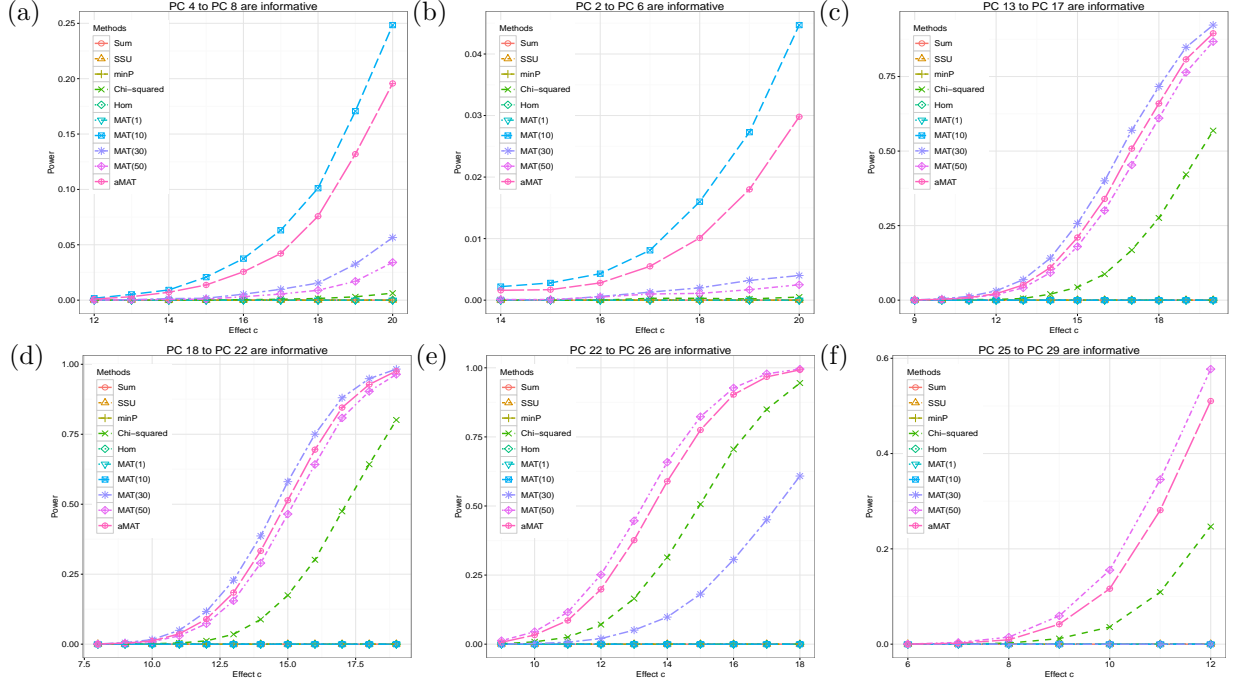


Figure S4: **Empirical power comparison with true Volume trait correlation matrix.** Under the alternative, we generated $\Delta = \sum_j c u_j$, where u_j is the singular vector of the Volume correlation matrix \mathbf{R} , c is the effect size. Empirical power was estimated as the proportions of p -values less than significance level 5×10^{-8} . Competing methods including SUM [1], SSU [2, 3], Chi-squared test, Hom [4] test, MAT(1) [5], and minP test [6] have been briefly described in Methods.

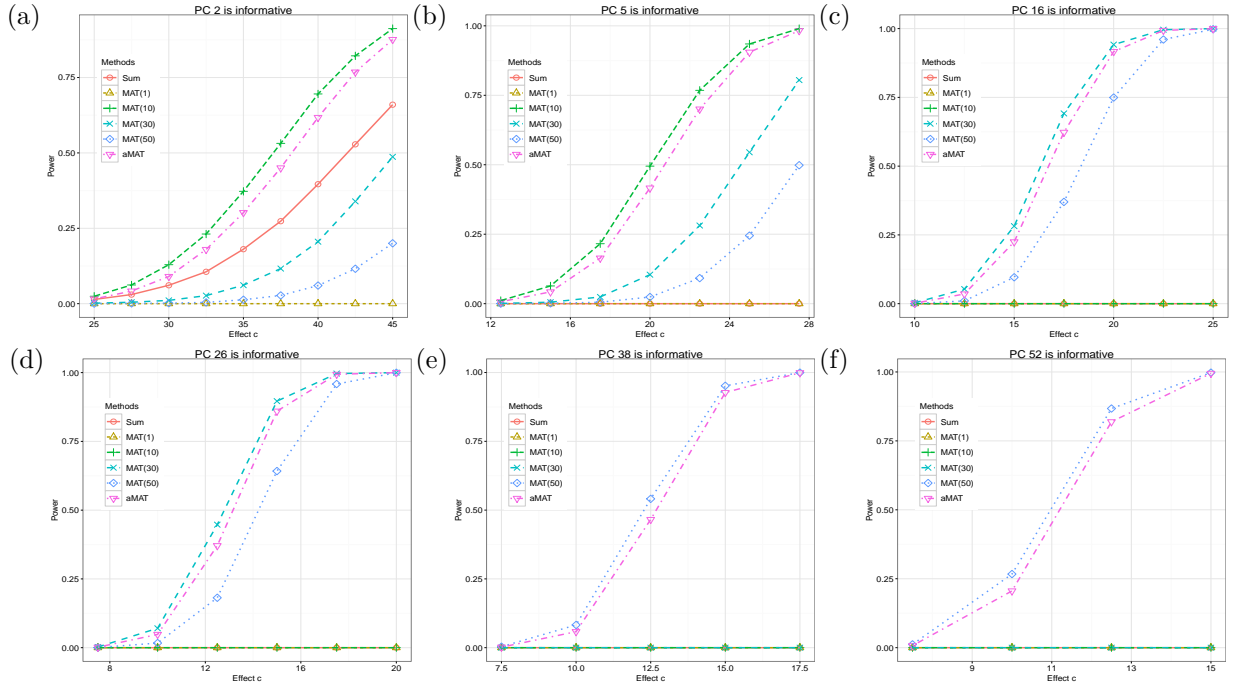


Figure S5: **Empirical power comparison with true Freesurf trait correlation matrix.** Under the alternative, we generated $\Delta = cu_j$, where u_j is the singular vector of the Volume correlation matrix \mathbf{R} , c is the effect size. Empirical power was estimated as the proportions of p -values less than significance level 5×10^{-8} .

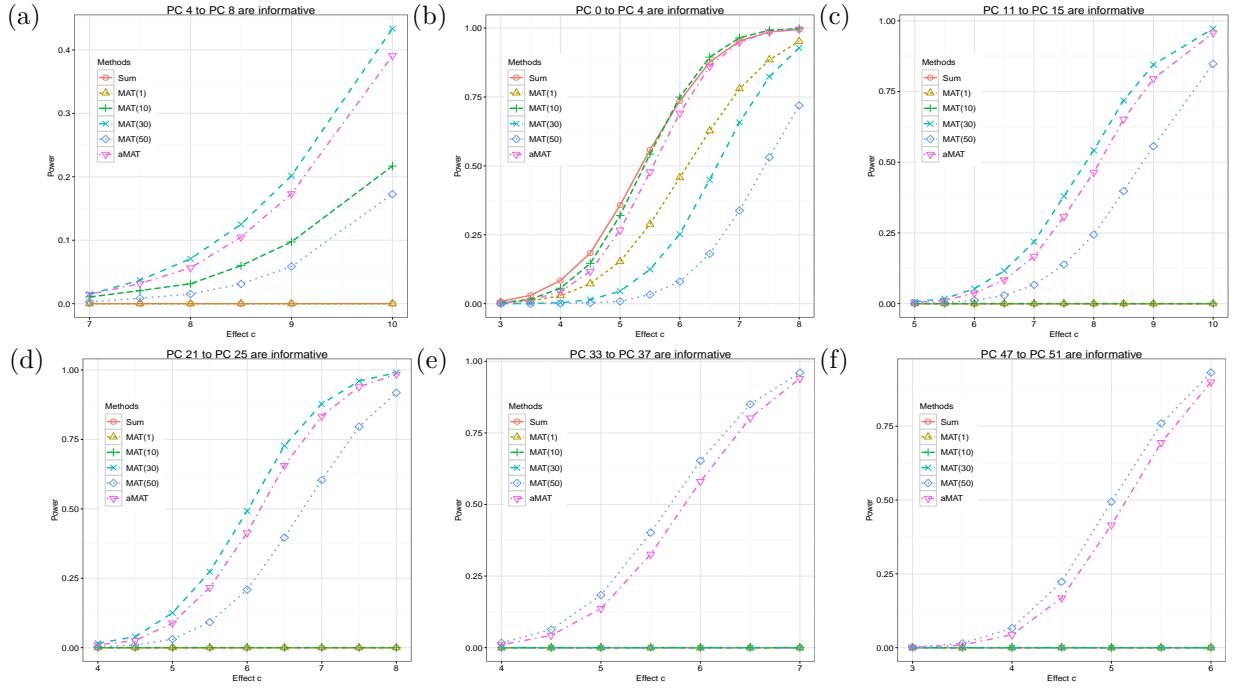


Figure S6: **Empirical power comparison with true Freesurf trait correlation matrix.** Under the alternative, we generated $\Delta = \sum_j c u_j$, where u_j is the singular vector of the Volume correlation matrix \mathbf{R} , c is the effect size. Empirical power was estimated as the proportions of p -values less than significance level 5×10^{-8} .

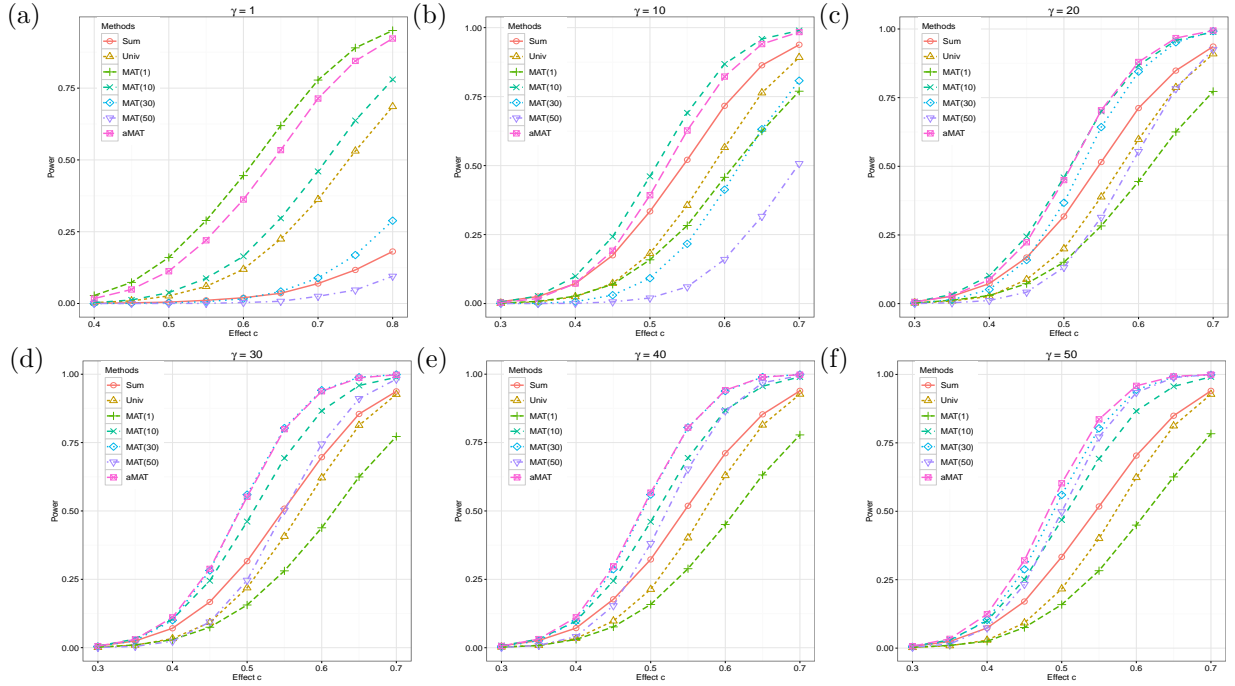


Figure S7: **Empirical power comparison with true Freesurf trait correlation matrix.** Under the alternative, we generated $\Delta = \sum_{j=1}^k c\sigma_j u_j$, where u_j is the informative singular vector of the Volume correlation matrix \mathbf{R} , c is the effect size, and k is the largest integer that stratifies $\sigma_1/\sigma_k < \gamma$. Empirical power was estimated as the proportions of p -values less than significance level 5×10^{-8} .

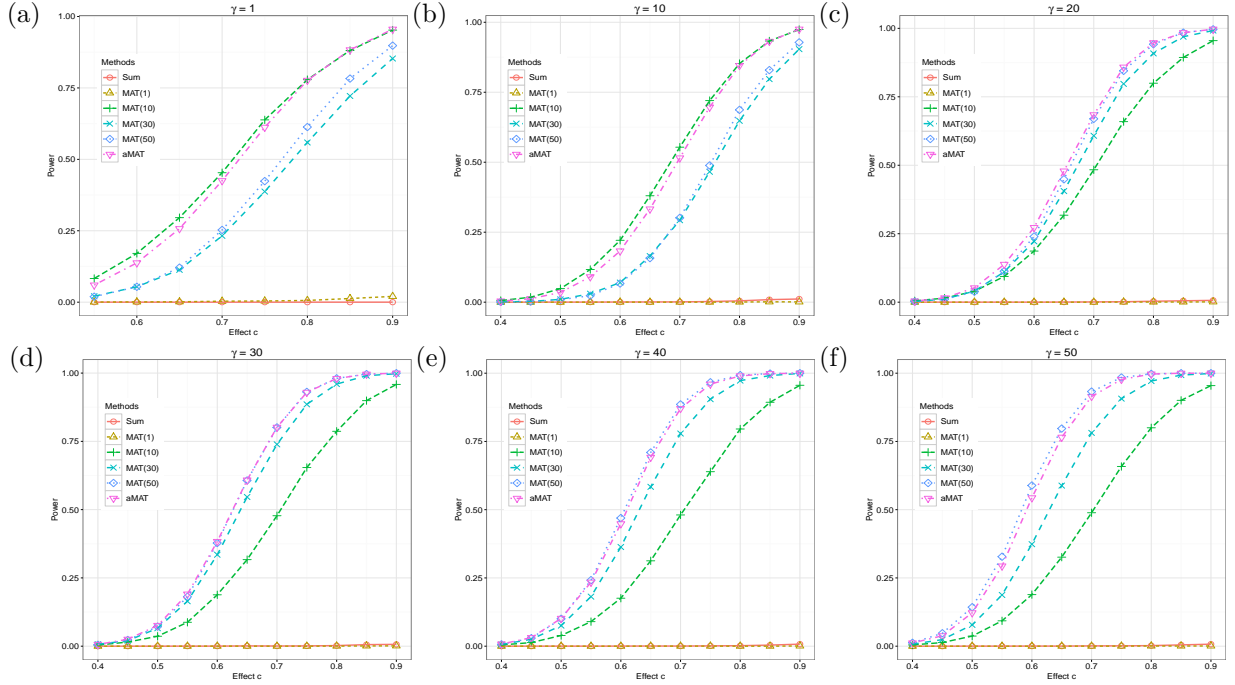


Figure S8: **Empirical power comparison with true Freesurf trait correlation matrix.** Under the alternative, we generated $\Delta = \sum_{j=1}^k c\sigma_j u_j$, where u_j is the informative singular vector of the Volume correlation matrix \mathbf{R} , c is the effect size, and k is the largest integer that stratifies $\sigma_1/\sigma_k < \gamma$. We further randomly chose 30% of Δ to be zero. Empirical power was estimated as the proportions of p -values less than significance level 5×10^{-8} .

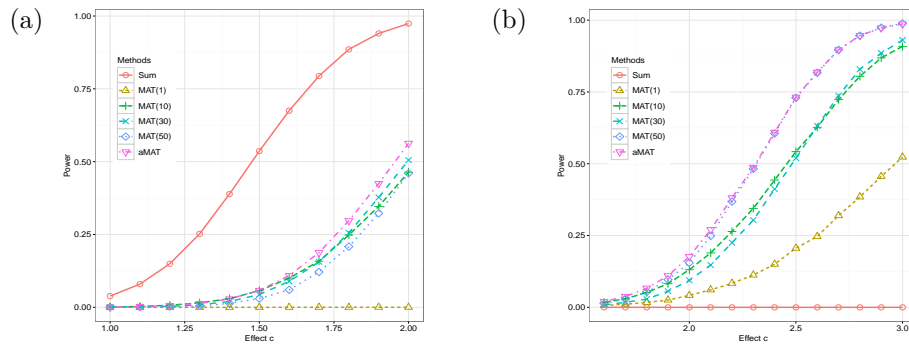


Figure S9: **Empirical power comparison with true Freesurf trait correlation matrix.** Under the alternative, we generated $\Delta = c$, where c is the effect size for subfigure a, and generated half of Δ from a uniform distribution $U(0, c)$ while the half from a uniform distribution $U(-c, 0)$ for subfigure b. Empirical power was estimated as the proportions of p -values less than significance level 5×10^{-8} .

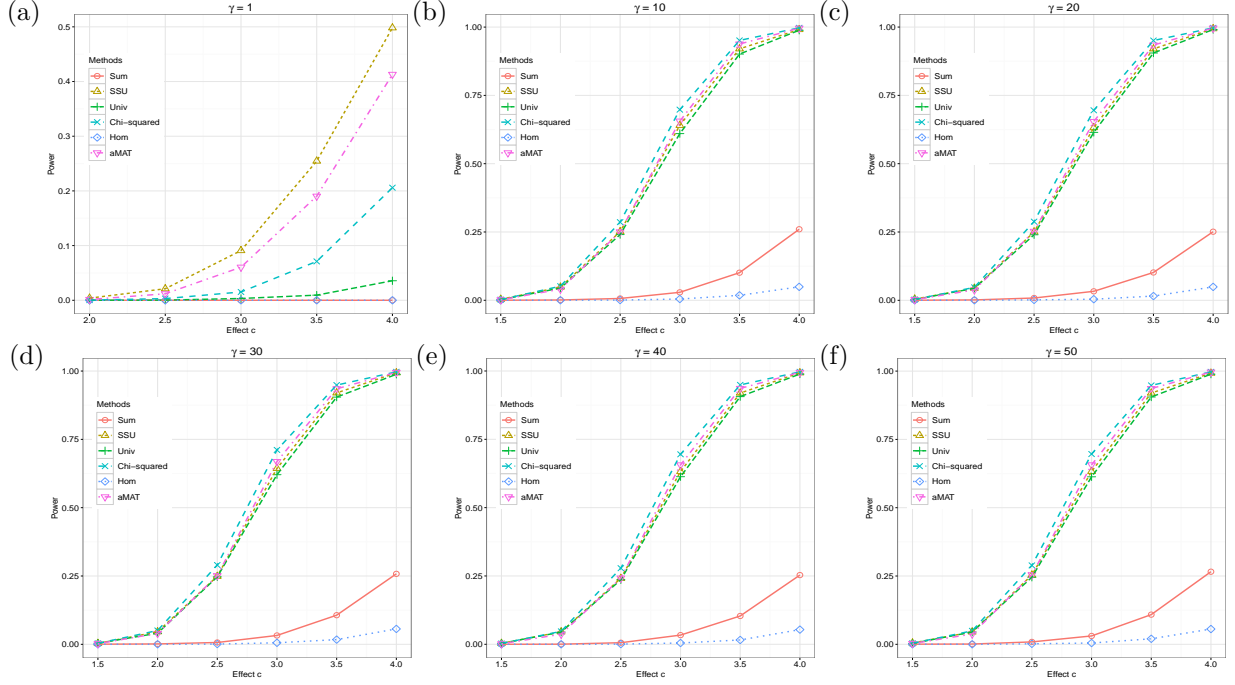


Figure S10: **Empirical power comparison with a five traits correlation matrix.** We randomly select five traits from the volumetric trait matrix and assume the true trait correlation matrix is known. Under the alternative, we generated $\Delta = \sum_{j=1}^k c\sigma_j u_j$, where u_j is the informative singular vector of the Volume correlation matrix \mathbf{R} , c is the effect size, and k is the largest integer that stratifies $\sigma_1/\sigma_k < \gamma$. Empirical power was estimated as the proportions of p -values less than significance level 5×10^{-8} .

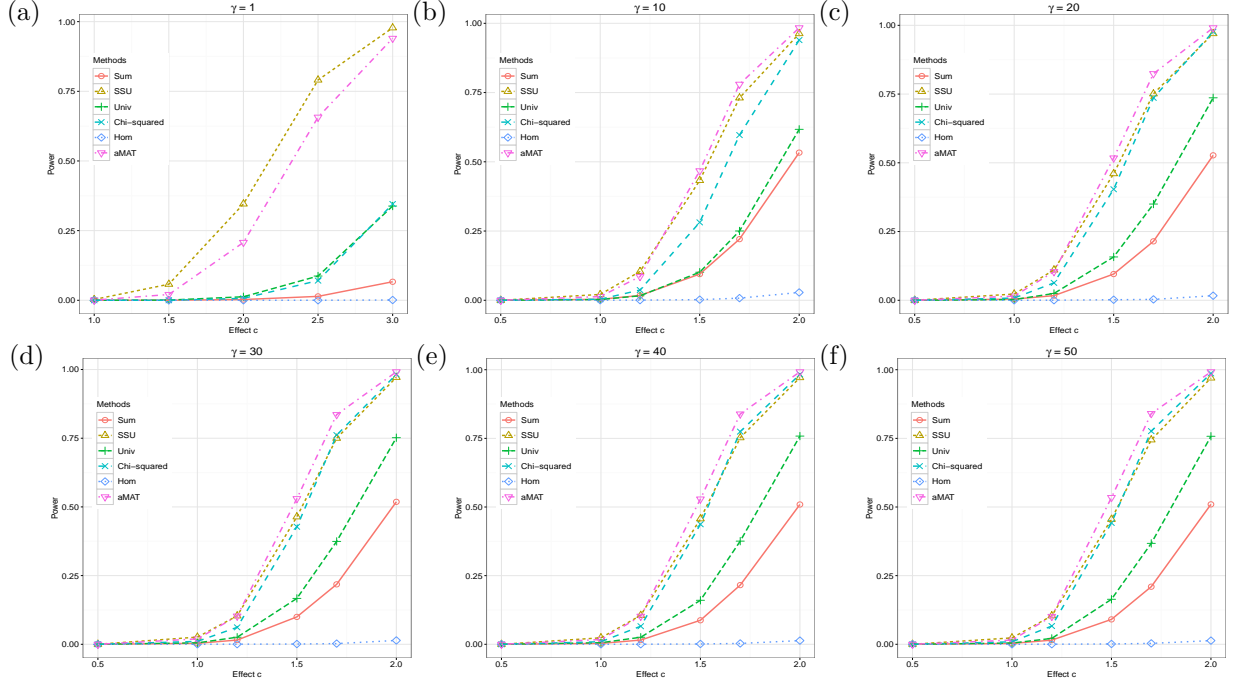


Figure S11: **Empirical power comparison with a twenty-five traits correlation matrix.** We randomly select 25 traits from the volumetric trait matrix and assume the true trait correlation matrix is known. Under the alternative, we generated $\Delta = \sum_{j=1}^k c\sigma_j u_j$, where u_j is the informative singular vector of the Volume correlation matrix \mathbf{R} , c is the effect size, and k is the largest integer that stratifies $\sigma_1/\sigma_k < \gamma$. Empirical power was estimated as the proportions of p -values less than significance level 5×10^{-8} .

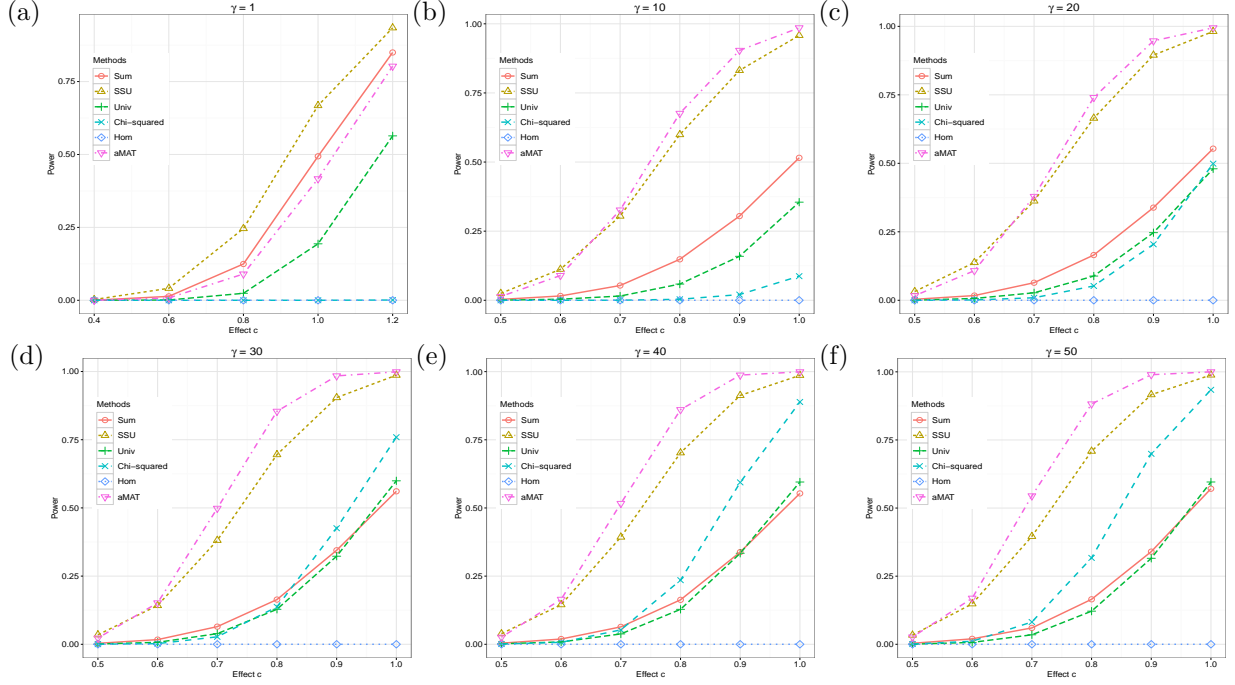


Figure S12: **Empirical power comparison with true Freesurf area-based trait correlation matrix.** This trait correlation matrix contains 206 IDPs. Under the alternative, we generated $\Delta = \sum_{j=1}^k c\sigma_j u_j$, where u_j is the informative singular vector of the Volume correlation matrix \mathbf{R} , c is the effect size, and k is the largest integer that stratifies $\sigma_1/\sigma_k < \gamma$. We further randomly chose 30% of Δ to be zero. Empirical power was estimated as the proportions of p -values less than significance level 5×10^{-8} .

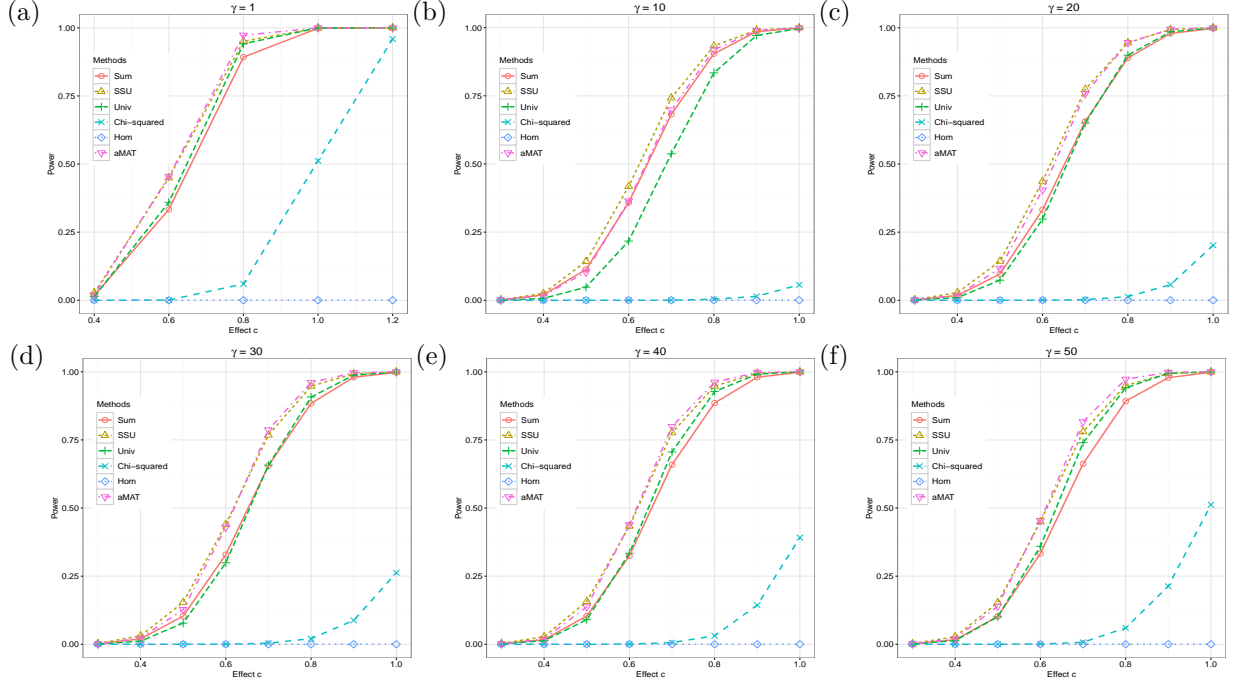


Figure S13: **Empirical power comparison with true Freesurf thickness-based trait correlation matrix.** This trait correlation matrix contains 208 IDPs. Under the alternative, we generated $\Delta = \sum_{j=1}^k c\sigma_j u_j$, where u_j is the informative singular vector of the Volume correlation matrix \mathbf{R} , c is the effect size, and k is the largest integer that stratifies $\sigma_1/\sigma_k < \gamma$. We further randomly chose 30% of Δ to be zero. Empirical power was estimated as the proportions of p -values less than significance level 5×10^{-8} .

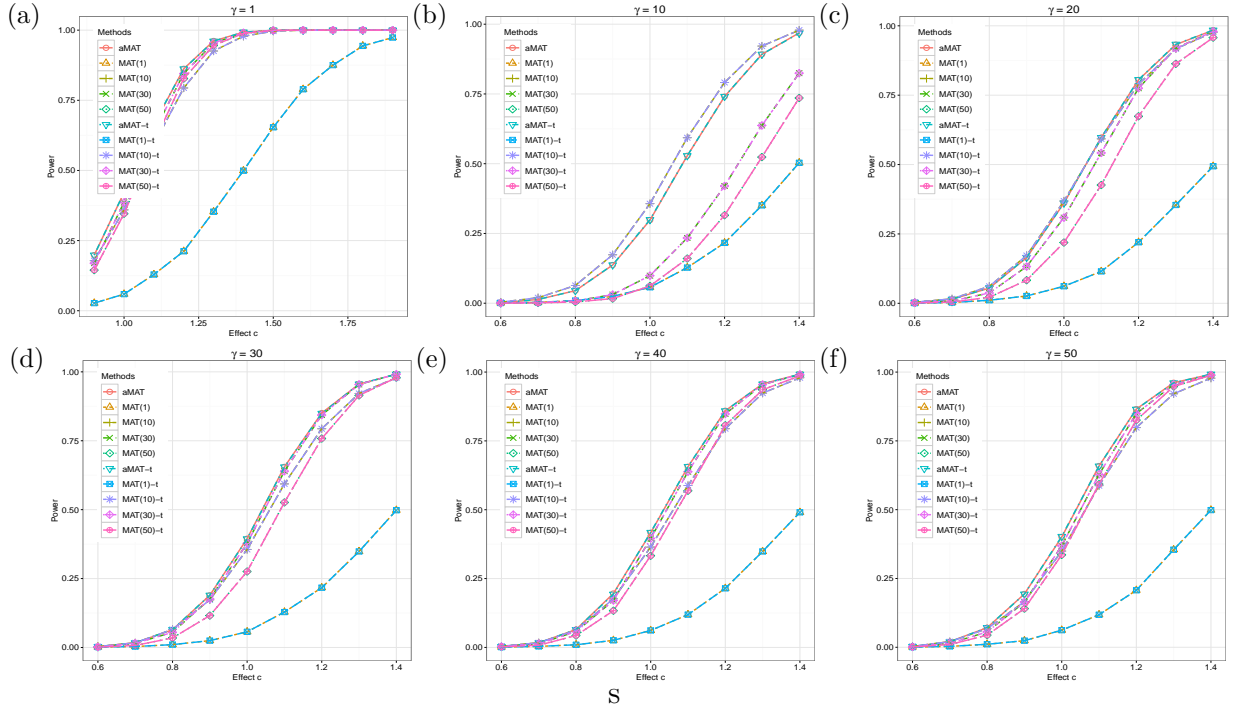


Figure S14: **Empirical power comparison between true and estimated Volume trait correlation matrix.** Under the alternative, we generated $\Delta = \sum_{j=1}^k c\sigma_j u_j$, where u_j is the singular vector of the true Volume correlation matrix \mathbf{R} , c is the effect size and k is the largest integer that stratifies $\sigma_1/\sigma_k < \gamma$. We simulated 10,000 replications with \mathbf{R} under the null and constructed test statistics with $\hat{\mathbf{R}}(10^{-5})$. We further estimated empirical power as the proportions of p -values less than significance level 5×10^{-8} . MAT(1), MAT(10), MAT(30), MAT(50), aMAT represent the results with $\hat{\mathbf{R}}(10^{-5})$, while MAT(1)-t, MAT(10)-t, MAT(30)-t, MAT(50)-t, aMAT-t represent the results with \mathbf{R} .

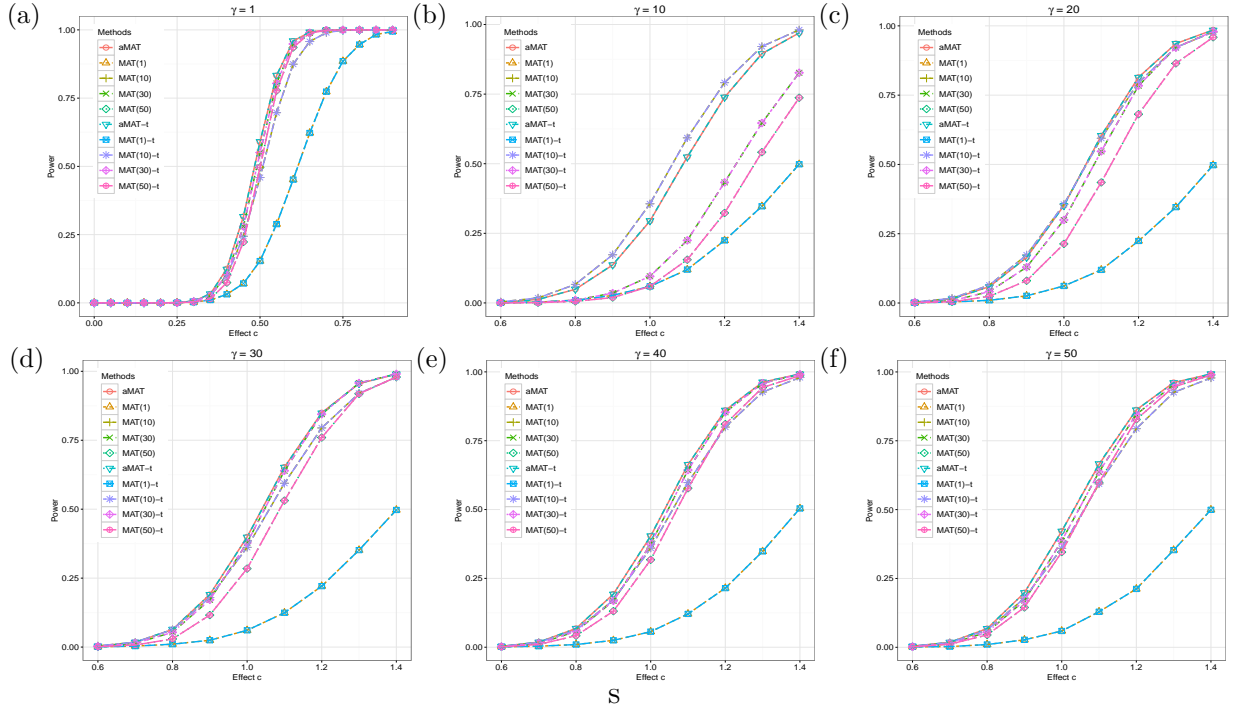


Figure S15: **Empirical power comparison between true and estimated Volume trait correlation matrix.** Under the alternative, we generated $\Delta = \sum_{j=1}^k c\sigma_j u_j$, where u_j is the singular vector of the true Volume correlation matrix \mathbf{R} , c is the effect size and k is the largest integer that stratifies $\sigma_1/\sigma_k < \gamma$. We simulated 10,000 replications with \mathbf{R} under the null and constructed test statistics with $\hat{\mathbf{R}}(5 \times 10^{-5})$. We further estimated empirical power as the proportions of p -values less than significance level 5×10^{-8} . MAT(1), MAT(10), MAT(30), MAT(50), aMAT represent the results with $\hat{\mathbf{R}}(5 \times 10^{-5})$, while MAT(1)-t, MAT(10)-t, MAT(30)-t, MAT(50)-t, aMAT-t represent the results with \mathbf{R} .

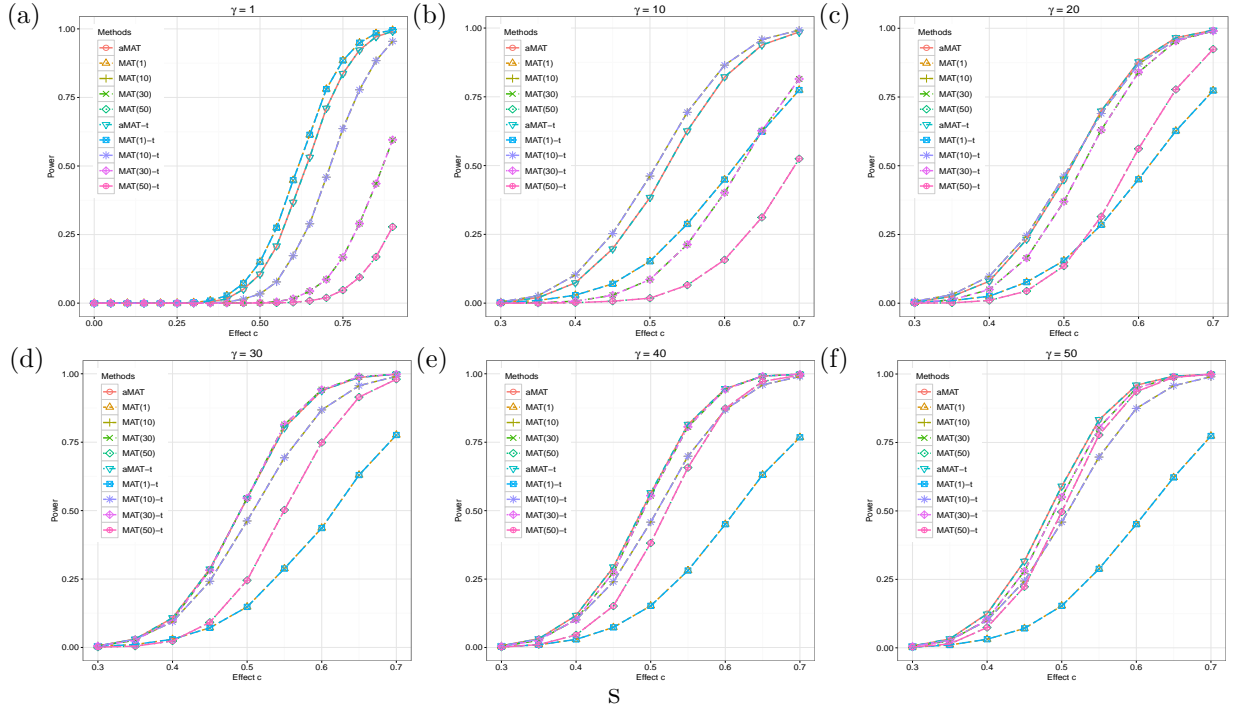


Figure S16: **Empirical power comparison between true and estimated Freesurf trait correlation matrix.** Under the alternative, we generated $\Delta = \sum_{j=1}^k c\sigma_j u_j$, where u_j is the singular vector of the true Freesurf correlation matrix \mathbf{R} , c is the effect size and k is the largest integer that stratifies $\sigma_1/\sigma_k < \gamma$. We simulated 10,000 replications with \mathbf{R} under the null and constructed test statistics with $\hat{\mathbf{R}}(10^{-5})$. We further estimated empirical power as the proportions of p -values less than significance level 5×10^{-8} . MAT(1), MAT(10), MAT(30), MAT(50), aMAT represent the results with $\hat{\mathbf{R}}(10^{-5})$, while MAT(1)-t, MAT(10)-t, MAT(30)-t, MAT(50)-t, aMAT-t represent the results with \mathbf{R} .

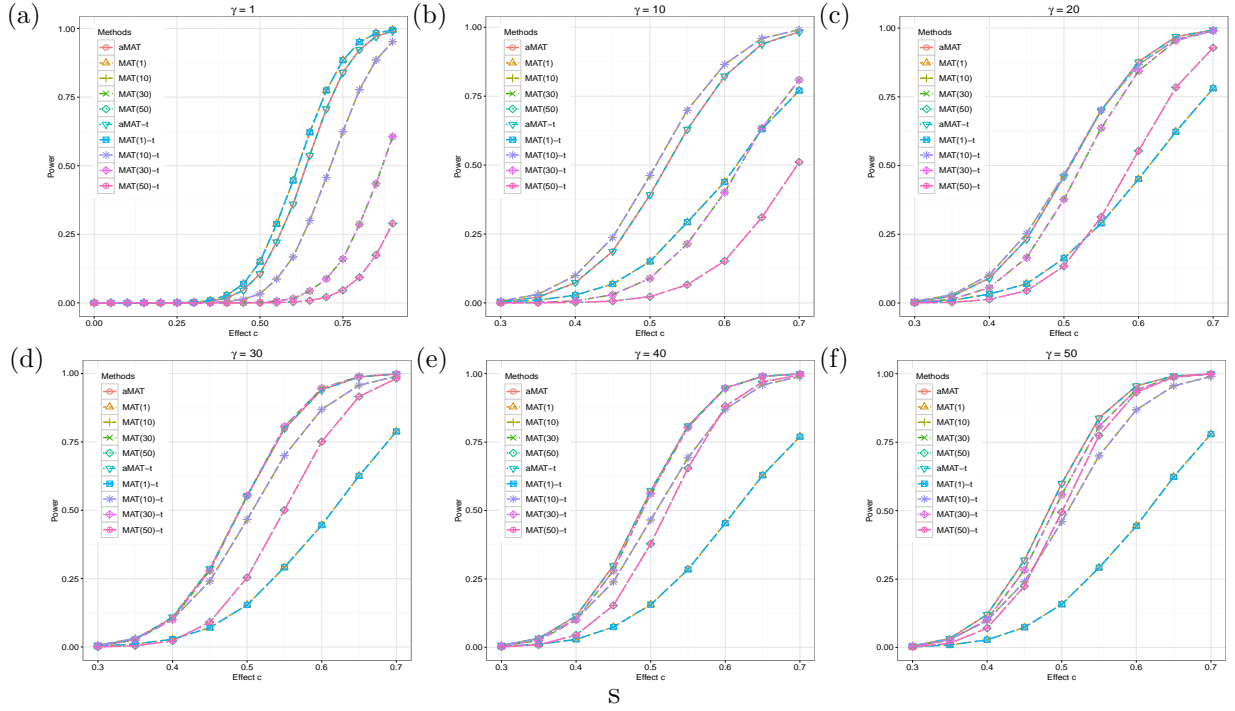


Figure S17: **Empirical power comparison between true and estimated Freesurf trait correlation matrix.** Under the alternative, we generated $\Delta = \sum_{j=1}^k c\sigma_j u_j$, where u_j is the singular vector of the true Freesurf correlation matrix \mathbf{R} , c is the effect size and k is the largest integer that stratifies $\sigma_1/\sigma_k < \gamma$. We simulated 10,000 replications with \mathbf{R} under the null and constructed test statistics with $\hat{\mathbf{R}}(5 \times 10^{-5})$. We further estimated empirical power as the proportions of p -values less than significance level 5×10^{-8} . MAT(1), MAT(10), MAT(30), MAT(50), aMAT represent the results with $\hat{\mathbf{R}}(5 \times 10^{-5})$, while MAT(1)-t, MAT(10)-t, MAT(30)-t, MAT(50)-t, aMAT-t represent the results with \mathbf{R} .

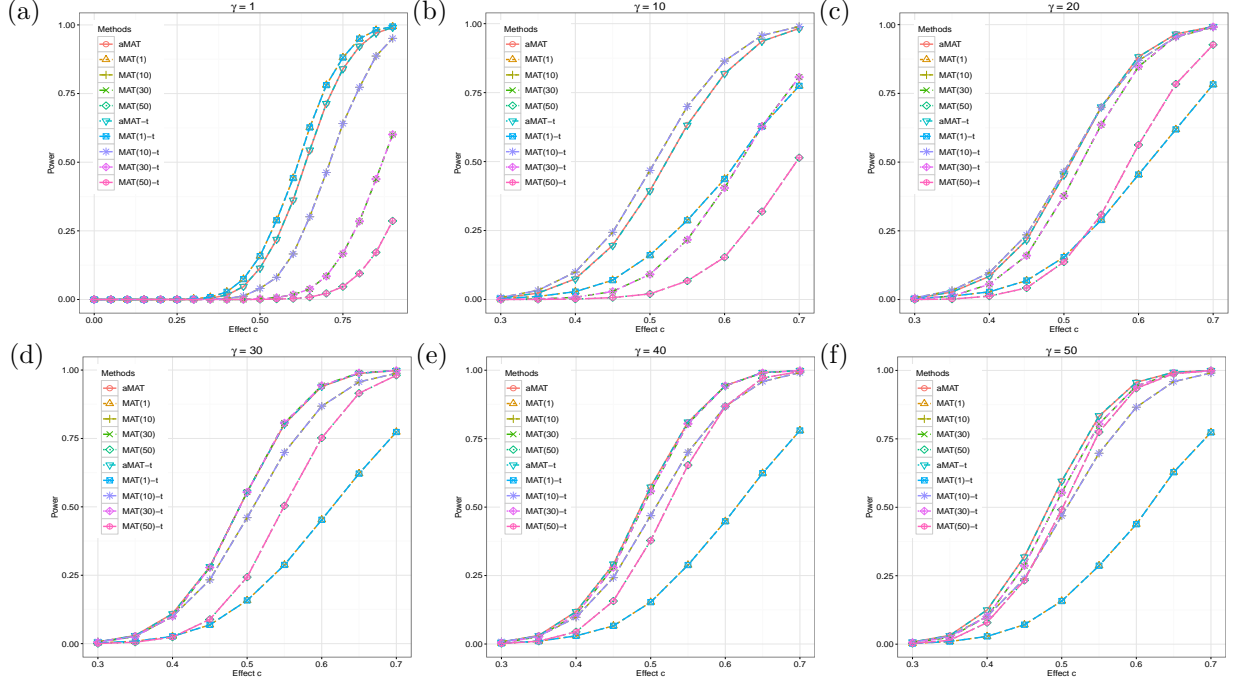


Figure S18: **Empirical power comparison between true and estimated Freesurf trait correlation matrix.** Under the alternative, we generated $\Delta = \sum_{j=1}^k c\sigma_j u_j$, where u_j is the singular vector of the true Freesurf correlation matrix \mathbf{R} , c is the effect size and k is the largest integer that stratifies $\sigma_1/\sigma_k < \gamma$. We simulated 10,000 replications with \mathbf{R} under the null and constructed test statistics with $\hat{\mathbf{R}}(10^{-4})$. We further estimated empirical power as the proportions of p -values less than significance level 5×10^{-8} . MAT(1), MAT(10), MAT(30), MAT(50), aMAT represent the results with $\hat{\mathbf{R}}(10^{-4})$, while MAT(1)-t, MAT(10)-t, MAT(30)-t, MAT(50)-t, aMAT-t represent the results with \mathbf{R} .

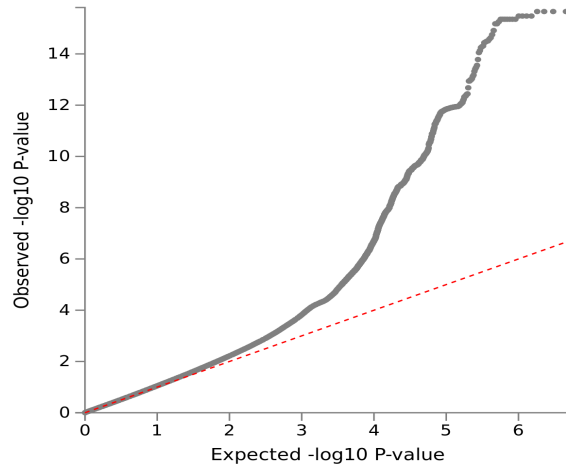


Figure S19: **QQ plot of the aMAT results for analyzing the Volume group.** The genomic inflation factor is 1.04.

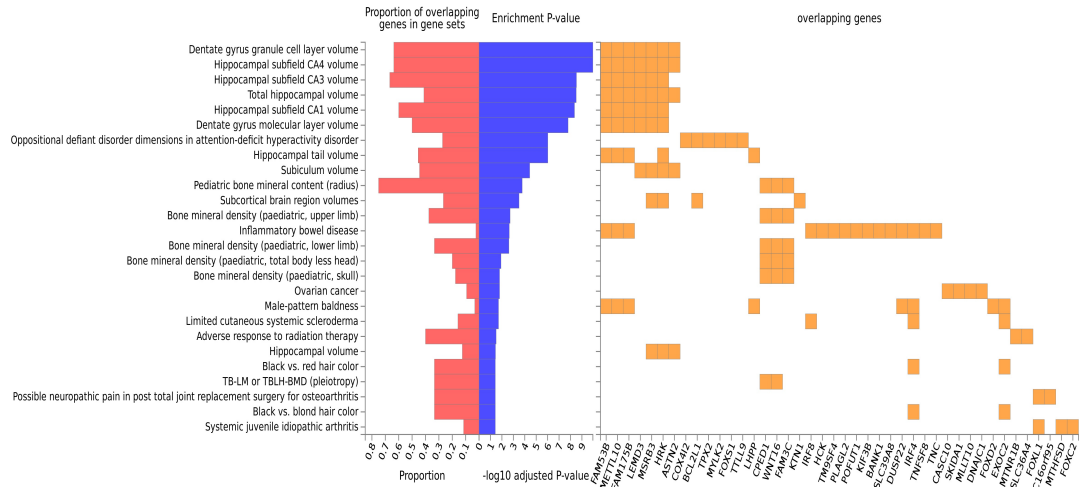


Figure S20: **Gene set enrichment analysis for FUMA mapped genes.** aMAT identified SNPs for the Volume group were mapped to genes by FUMA. Hypergeometric tests were performed to test if the mapped genes are overrepresented in the pre-defined gene sets from the GWAS-catalog.

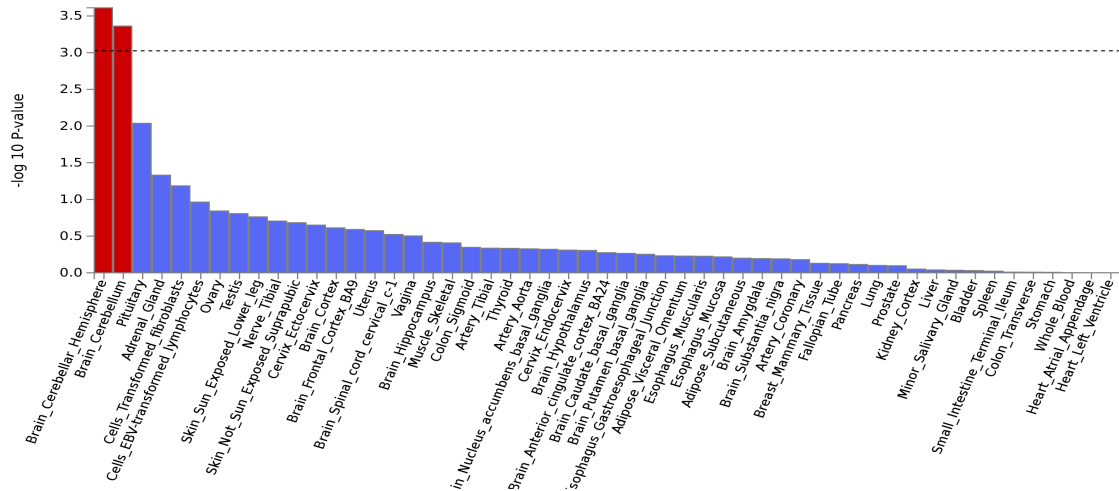


Figure S21: **MAGMA tissue expression analysis for FUMA mapped genes.** aMAT identified SNPs for the Volume group were mapped to genes by FUMA. MAGMA tissue expression analysis was conducted to test whether the mapped genes are enriched in a tissue. The dashed line represents the Bonferroni correction cutoff.

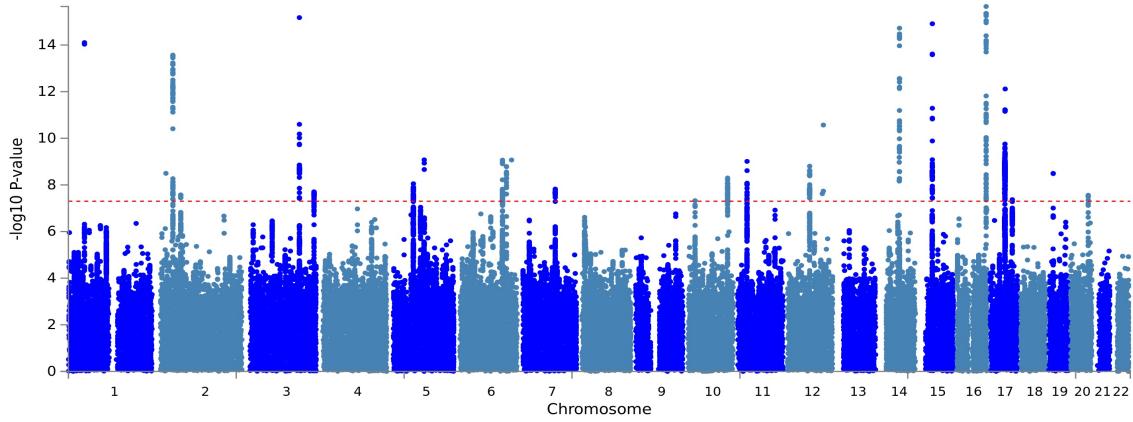


Figure S22: **Multi-trait analysis for the Area group.** Manhattan plot displays the association results of aMAT per variant ordered by their genomic position on the x axis and showing the strength with the $-\log_{10}(p)$ on the y axis.

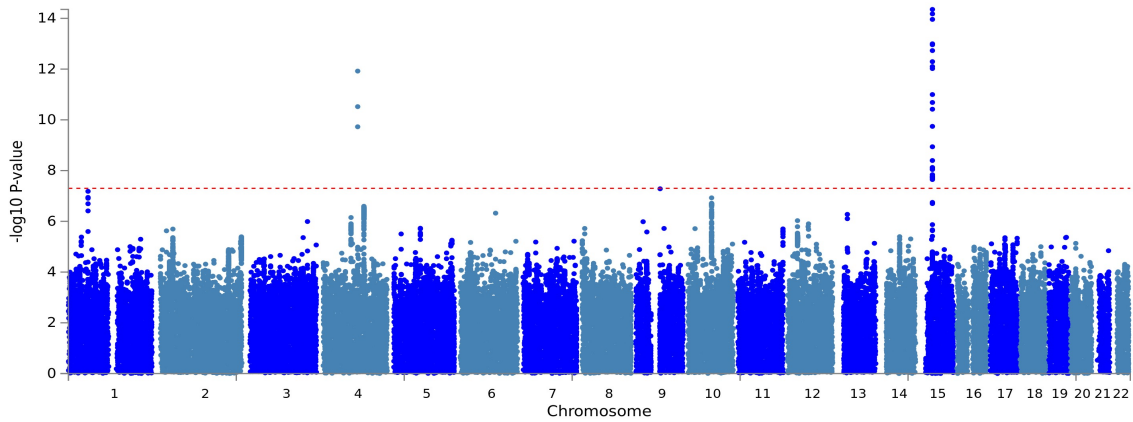


Figure S23: **Multi-trait analysis for the Thickness group.** Manhattan plot displays the association results of aMAT per variant ordered by their genomic position on the x axis and showing the strength with the $-\log_{10}(p)$ on the y axis.

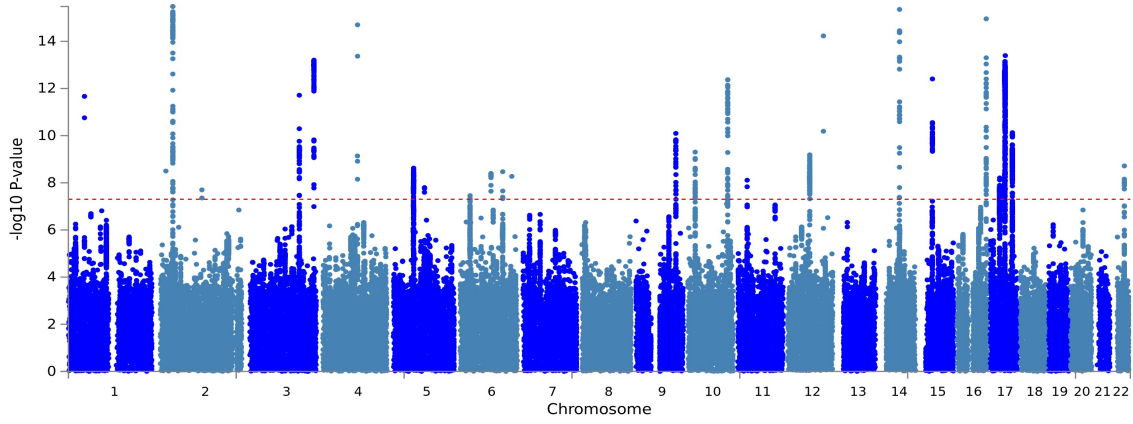


Figure S24: **Multi-trait analysis for the Freesurf group.** Manhattan plot displays the association results of aMAT per variant ordered by their genomic position on the x axis and showing the strength with the $-\log_{10}(p)$ on the y axis.

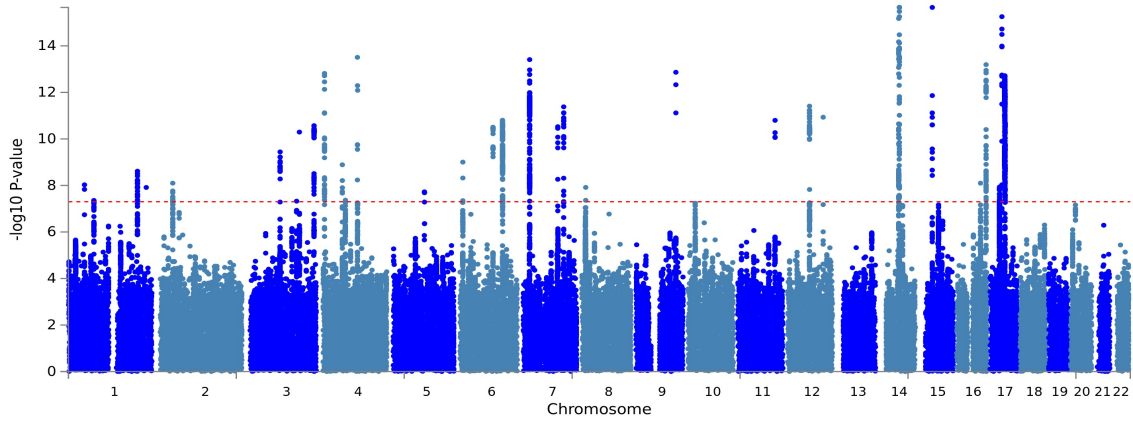
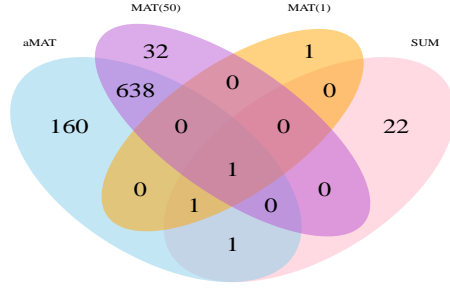
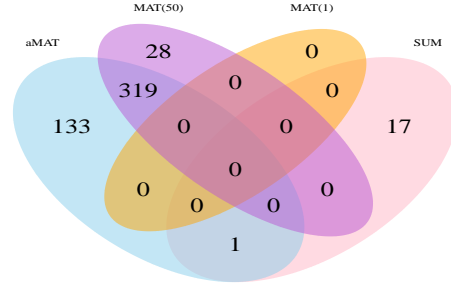


Figure S25: **Multi-trait analysis for the ROIs group.** Manhattan plot displays the association results of aMAT per variant ordered by their genomic position on the x axis and showing the strength with the $-\log_{10}(p)$ on the y axis.

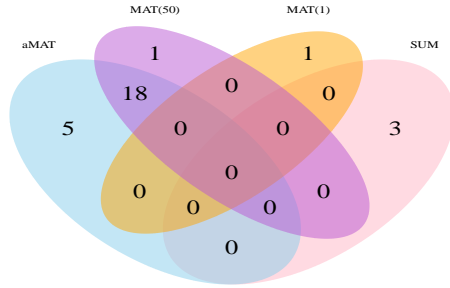
(a)



(b)



(c)



(d)

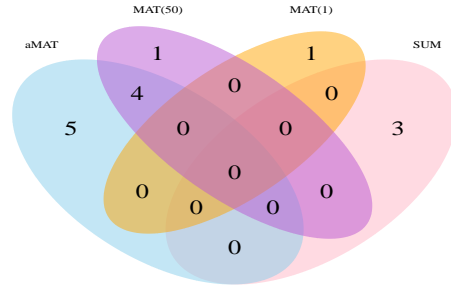
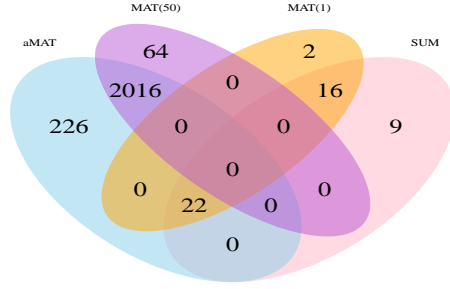
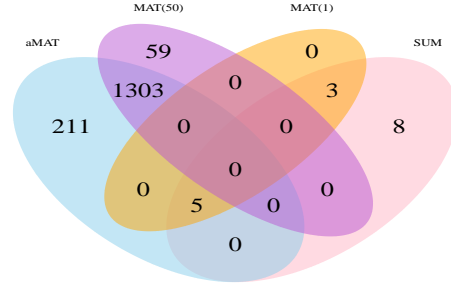


Figure S26: **Methods comparison based on the Volume IDPs data.** (a) Venn diagram of number of significantly associated SNPs identified by different methods. (b) Venn diagram of the number of significant and novel SNPs identified by different methods. A significant and novel SNP is defined as one that is significant and not detected by any individual IDP tests at the 5×10^{-8} genome-wide significance level. (c) Venn diagram of the number of significant risk regions identified by different methods. (d) Venn diagram of the number of significant and novel risk regions identified by different methods. A significant and novel risk region is defined as one that is significant and not detected by any individual IDP tests at the 5×10^{-8} genome-wide significance level.

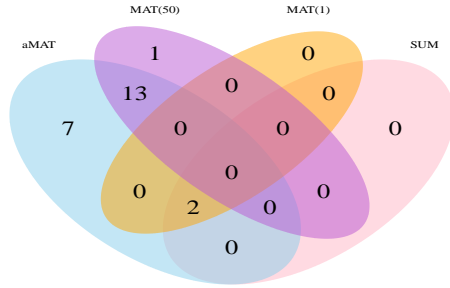
(a)



(b)



(c)



(d)

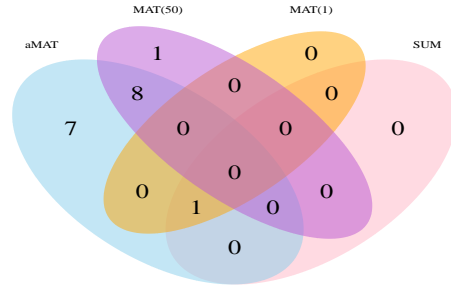
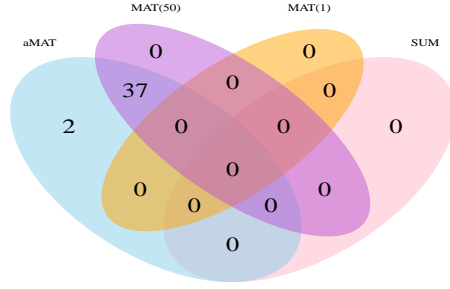
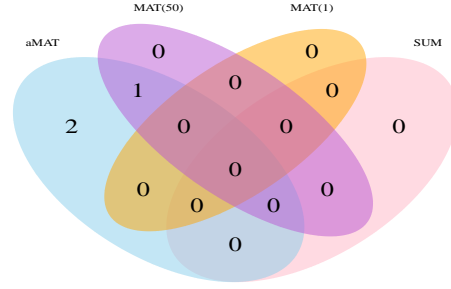


Figure S27: **Methods comparison based on the Area IDPs data.** (a) Venn diagram of number of significantly associated SNPs identified by different methods. (b) Venn diagram of the number of significant and novel SNPs identified by different methods. A significant and novel SNP is defined as one that is significant and not detected by any individual IDP tests at the 5×10^{-8} genome-wide significance level. (c) Venn diagram of the number of significant risk regions identified by different methods. (d) Venn diagram of the number of significant and novel risk regions identified by different methods. A significant and novel risk region is defined as one that is significant and not detected by any individual IDP tests at the 5×10^{-8} genome-wide significance level.

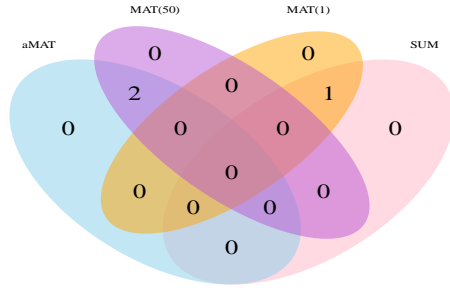
(a)



(b)



(c)



(d)

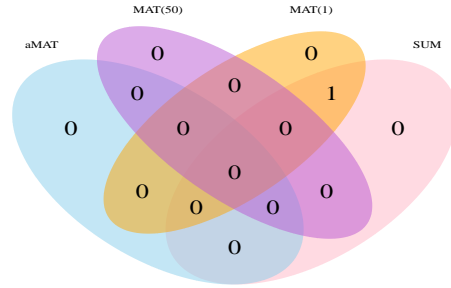
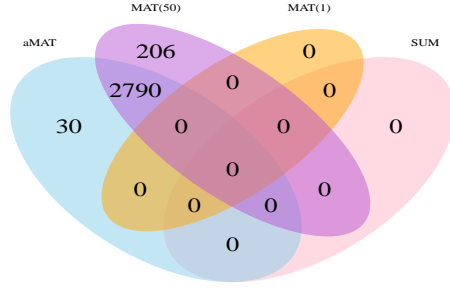
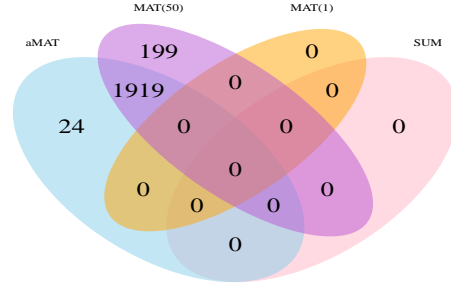


Figure S28: **Methods comparison based on the Thickness IDPs data.** (a) Venn diagram of number of significantly associated SNPs identified by different methods. (b) Venn diagram of the number of significant and novel SNPs identified by different methods. A significant and novel SNP is defined as one that is significant and not detected by any individual IDP tests at the 5×10^{-8} genome-wide significance level. (c) Venn diagram of the number of significant risk regions identified by different methods. (d) Venn diagram of the number of significant and novel risk regions identified by different methods. A significant and novel risk region is defined as one that is significant and not detected by any individual IDP tests at the 5×10^{-8} genome-wide significance level.

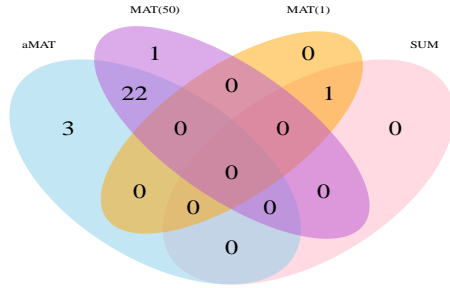
(a)



(b)



(c)



(d)

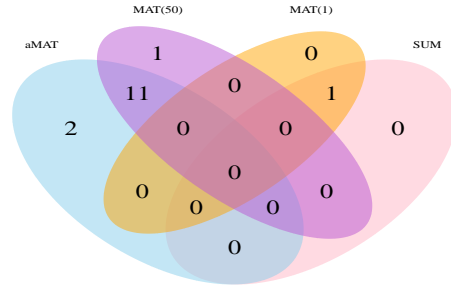
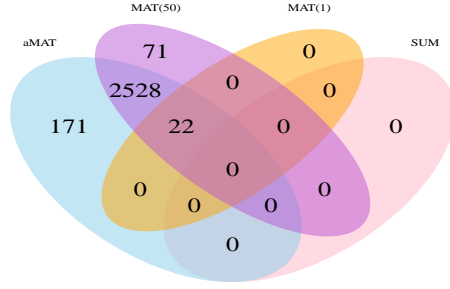
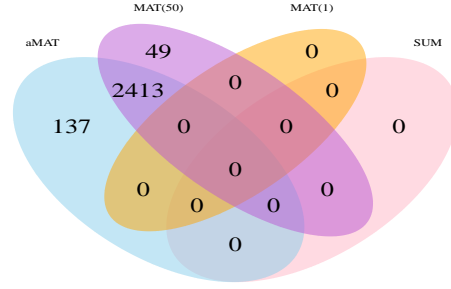


Figure S29: **Methods comparison based on the Freesurf IDPs data.** (a) Venn diagram of number of significantly associated SNPs identified by different methods. (b) Venn diagram of the number of significant and novel SNPs identified by different methods. A significant and novel SNP is defined as one that is significant and not detected by any individual IDP tests at the 5×10^{-8} genome-wide significance level. (c) Venn diagram of the number of significant risk regions identified by different methods. (d) Venn diagram of the number of significant and novel risk regions identified by different methods. A significant and novel risk region is defined as one that is significant and not detected by any individual IDP tests at the 5×10^{-8} genome-wide significance level.

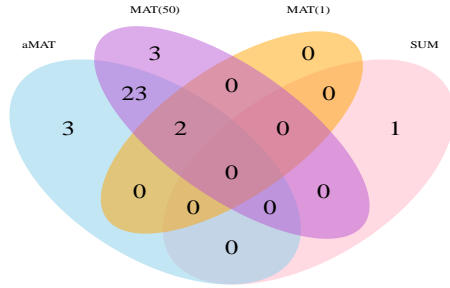
(a)



(b)



(c)



(d)

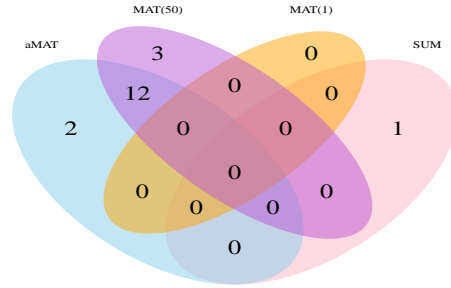


Figure S30: **Methods comparison based on the ROIs IDPs data.** (a) Venn diagram of number of significantly associated SNPs identified by different methods. (b) Venn diagram of the number of significant and novel SNPs identified by different methods. A significant and novel SNP is defined as one that is significant and not detected by any individual IDP tests at the 5×10^{-8} genome-wide significance level. (c) Venn diagram of the number of significant risk regions identified by different methods. (d) Venn diagram of the number of significant and novel risk regions identified by different methods. A significant and novel risk region is defined as one that is significant and not detected by any individual IDP tests at the 5×10^{-8} genome-wide significance level.

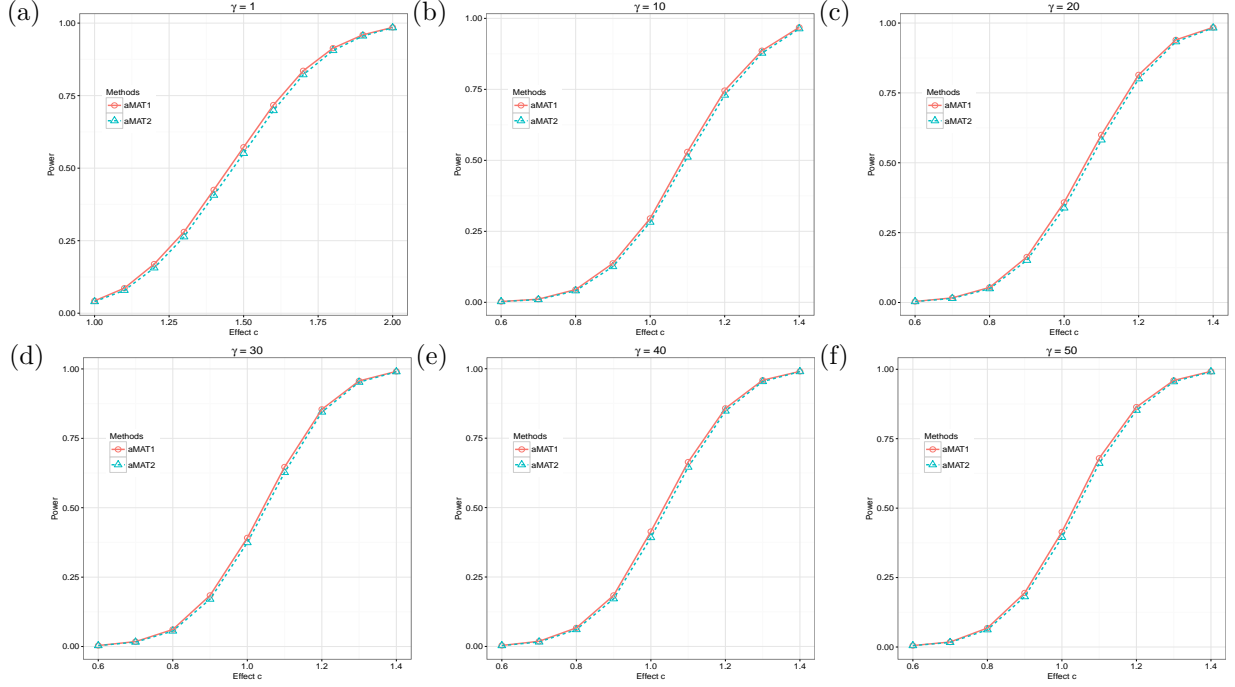


Figure S31: **Empirical power comparison with true Volume trait correlation matrix.** Under the alternative, we generated $\Delta = \sum_{j=1}^k c\sigma_j u_j$, where u_j is the singular vector of the Volume correlation matrix \mathbf{R} , c is the effect size and k is the largest integer that stratifies $\sigma_1/\sigma_k < \gamma$. We further estimated empirical power as the proportions of p -values less than significance level 5×10^{-8} . aMAT1 and aMAT represent the results of aMAT with $\Gamma = \{1, 10, 30, 50\}$ and with $\Gamma = \{1, 10, 20, 30, 40, 50\}$, respectively.

References

- [1] He Q, Avery CL, Lin DY. A general framework for association tests with multivariate traits in large-scale genomics studies. *Genetic Epidemiology*. 2013;37(8):759–767.
- [2] Pan W. Asymptotic tests of association with multiple SNPs in linkage disequilibrium. *Genetic Epidemiology*. 2009;33(6):497–507.
- [3] Yang Q, Wang Y. Methods for analyzing multivariate phenotypes in genetic association studies. *Journal of Probability and Statistics*. 2012;2012:652569.
- [4] Zhu X, Feng T, Tayo BO, Liang J, Young JH, Franceschini N, et al. Meta-analysis of correlated traits via summary statistics from GWASs with an application in hypertension. *The American Journal of Human Genetics*. 2015;96(1):21–36.
- [5] Guo B, Wu B. Integrate multiple traits to detect novel trait–gene association using GWAS summary data with an adaptive test approach. *Bioinformatics*. 2018;.
- [6] Conneely KN, Boehnke M. So many correlated tests, so little time! Rapid adjustment of P values for multiple correlated tests. *The American Journal of Human Genetics*. 2007;81(6):1158–1168.